



## Kinetic, Isothermal and Thermodynamic Investigations for The Use of Pumpkin Seed Husks as Low-Cost Biosorbent of Solochrome Cyanine R from Aqueous Solutions



**Saddam Mohammed Al-Mahmoud**

*Department of Chemistry, College of Education for Women, Tikrit University, Tikrit, Iraq.*

**P**UMPKIN seed husks were used in this research as effective-cost material for the adsorption of Solochrome cyanine R from aqueous solutions. A good removal ability of Pumpkin seed husks was noticed during this study, and the optimal adsorption conditions were found to be 120 min. equilibrium contact time, 0.2 g biosorbent dosage, and 100 mg/L initial dye concentration. The kinetic investigation shows that applying the pseudo-second order model gives a better fit for the adsorption with the higher correlation coefficient. The isothermal investigation shows an excellent fit of data using the Langmuir model, and also predict that the removal process is favorable. The adsorption data at different temperatures were evaluated in order to obtain the thermodynamic parameters. The positive values of  $\Delta H^\circ$  and  $\Delta S^\circ$  indicate the endothermic and randomness of the adsorption process. Moreover, the negative values of  $\Delta G^\circ$  clarify that the adsorption process is spontaneous and more preferable at higher temperatures. Pumpkin seed husks as a low-cost biosorbent exhibit a great potential for the adsorption of Solochrome cyanine R from aqueous solutions.

**Keywords:** Pumpkin seed husks, Solochrome cyanine R, Adsorption.

### Introduction

Water contamination is a serious danger that can affect the lives of all human beings around the world. Organic and inorganic additives that used in the numerous industrial and agricultural applications can increase the pollution of the disposed water when it released to the aquatic environment without any effective treatment [1].

Dyes are the main additives that usually used in the textile industries. The existence of these colored materials in the discharged water from these industries is extremely unfavorable. It poses a threat and causes serious health problems due to its high toxicity [2]. Also, it can reduce the biological degradation due to the lack of sunlight entering to the water bodies [3]. Solochrome cyanine R (SCCR), also known as Eriochrome cyanine R and Chromoxane cyanine R is a pH indicator usually used in the acid-base titration

[4]. SCCR is a high soluble anionic dye, and it considers a very hazardous to the aquatic bodies due to its high resistance to the conventional water treatments [5].

Several treatment techniques such as adsorption, photocatalysis, biological treatment, ion exchange, coagulation, flocculation, Fenton, and membrane filtration, were employed to decrease the hazardous influences of these effluents from contaminated water [6–8]. Among all these techniques, adsorption is considered the most effective and preferred economical technique that has widely been used for wastewater treatment [9].

Numerous kinds of adsorbent materials have been commonly utilized for the removal of dyes effluents from wastewater, for example, activated carbon [10–13], metal oxides [14–16], clays [17–20]. Nowadays, great attention has been focused on discovering cost-effective and natural available

\*Corresponding author e-mail: [s\\_almahmoud@tu.edu.iq](mailto:s_almahmoud@tu.edu.iq), Tel: 009647702064603

Received 19/2/2020; Accepted 10/3/2020

DOI: 10.21608/ejchem.2020.24327.2445

©2020 National Information and Documentation Center (NIDOC)

adsorbents that can be used effectively for the treatment of wastewater. Many researchers have been used different Agricultural waste materials for the removal of various types of pollutants, such as banana and orange peels [21], Viscose waste [22], grapefruit peel [23], rice husk [24], sawdust [25], spent tea leaves [26], coconut [27], etc.

Pumpkin, an annual vegetable of the Cucurbitaceae family, is one of the important vegetables used widely around the world [28]. Its seed husks consider a great source of fiber [29], which can represent a good alternative as a low cost and naturally abundant biosorbent material for the removal of dyes from water.

In this research, several parameters including adsorbent dose, contact time, initial concentration, and temperature have been investigated. Also, three kinetic models had been introduced to understand the mechanism of the adsorption process. Kinetic investigation was described by fitting the experimental data to the pseudo-first order model [30], pseudo-second order model [31], and Intraparticle diffusion model [32]. The intraparticle diffusion model based on the theory developed by Weber and Morris is an interesting model to illustrate the diffusion mechanism [33]. The obtained results were analyzed and evaluated in order to study the effect of pumpkin seed husks (PSH) on the efficient removal of solochrome cyanine R from aqueous solutions.

## Materials and Methods

### Materials

Solochrome cyanine R (Fig. 1) was used as received from BDH Chemical Ltd (England) without any purification. Pumpkin seed was purchased from the local market in Mosul city in Iraq. It was peeled, and the husks were collected and washed several times with water and dried in

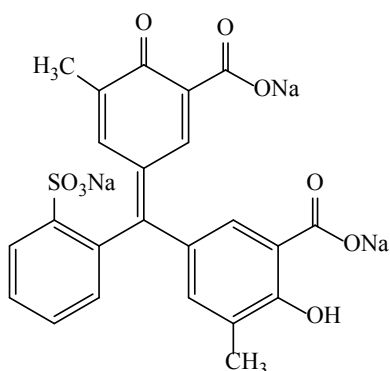


Fig.1. Chemical structure of Solochrome cyanine R.

the oven for 24 hr. at 85 °C. It was ground using a food grinder and sieved using molecular sieves (Retsch, Germany) to obtain small particles less than 20 µm. It was washed again with distilled water and dried for 24 hr. at 85 °C. The surface morphology of the PSH was characterized by field emission scanning electron microscopy (FESEM).

### Adsorption Experiments

In this study, the influence of the various parameters such as contact time (10-180 min), biosorbent dose (0.01-3.0 g), SCCR concentration (25-150 mg/L) and temperature (20-40 °C) on the adsorption of SCCR dye on PSH biosorbent from aqueous solutions was investigated. The adsorption experiments were conducted in a 100 ml conical flask with 25 ml of SCCR solution. Each solution was shaken using a shaking water bath (GFL, Germany) at a speed of 120 rpm under thermostatic condition in order to reach the adsorption equilibrium. After adsorption, each solution was centrifuged using (Gallenkamp centrifuge, England) at 2500 rpm for 5 min to obtain the supernatant that contains the residual SCCR concentration. The absorption measurements for the residual dye were carried out at 518 nm using a UV-Visible spectrophotometer (UV-1800, Shimadzu). The amount of the dye adsorbed on the surface of the biosorbent was then calculated from the concentration difference.

The pH of the dye solution has a significant effect on dye removal. It was already found that adsorption of SCCR was disfavoured in highly acidic and basic ranges [4], therefore all examined solutions were tested at a pH of (4.0), which considers the natural value of SCCR dye in the aqueous medium.

The adsorption percentage (% Adsorption), and the quantity of SCCR dye adsorbed per gram of PSH biosorbent  $qt$  (mg/g) were calculated using the following equations, respectively:

$$\% \text{ Removal Adsorption} = (C_0 - C_e) / C_0 \times 100 \quad (1)$$

$$qt = (C_0 - C_e) V / m \quad (2)$$

Where,  $C_0$  is the initial dye concentration (mg/L),  $C_e$  is the dye concentration (mg/L) at equilibrium,  $V$  is the volume of the dye solution (L), and  $m$  is the mass of the biosorbent (g).

The adsorption kinetics of the SCCR removal onto PSH was performed for the experimental data by applying three kinetic models, the

pseudo-first order model, pseudo-second order model, and Intraparticle diffusion model, whose linearized equations are presented in Eqs. (3) – (5), respectively [26, 33]:

$$\ln(q_e - q_t) = \ln q_e - k_1 t \quad (3)$$

$$t/q_t = (1/(k_2 q_e^2)) + (1/q_e) t \quad (4)$$

$$q_t = k_{int} t^{1/2} + C \quad (5)$$

Where  $q_e$  and  $q_t$  are the adsorption capacity (mg/g) at equilibrium and at time  $t$ , respectively.  $k_1$  is the pseudo-first order rate constant ( $\text{min}^{-1}$ ),  $k_2$  is the pseudo-second order rate constant ( $\text{g} \cdot \text{mg}^{-1} \cdot \text{min}^{-1}$ ),  $k_{int}$  is the intraparticle diffusion rate constant ( $\text{mg} \cdot \text{g}^{-1} \cdot \text{min}^{-1/2}$ ), and  $C$  is the intercept.

The isothermal investigation was carried using the Langmuir isotherm model [34]. The linear form of Langmuir isotherm can be represented in the following equation:

$$1/q_e = 1/q_m + (1/q_m K_L) 1/C_e \quad (6)$$

Where  $C_e$  (mg/L) the equilibrium concentration of the dye in solution,  $q_m$  (mg/g) a constant signifies the maximum adsorption capacity, and  $K_L$  (L/mg) is the Langmuir isotherm constant related to the energy required for the adsorption.

The thermodynamic parameters for the SCCR adsorption onto PSH were evaluated using the following equations [35]:

$$\Delta G^\circ = -RT \ln K_e \quad (7)$$

$$\Delta G^\circ = \Delta H^\circ - T\Delta S^\circ \quad (8)$$

$$\ln K_e = (\Delta S^\circ)/R - (\Delta H^\circ)/RT \quad (9)$$

Where,  $\Delta H^\circ$  is the standard enthalpy change (J/mol),  $\Delta S^\circ$  is the standard entropy change (J/mol K),  $\Delta G^\circ$  is the standard free energy change (J/mol),  $T$  is the absolute temperature (K),  $R$  is the gas constant (8.314 J/mol K).  $K_e$  is the distribution coefficient and can be obtained from the value  $K_L$  (L/mg) calculated from Langmuir isotherm by changing all concentrations to molar form and take into account the standard state of  $C^\circ$  equal to 1 mol/L as follows [17]:

$$K_e = K_L (L/mg) \times 1000 (mg/g) \times M_{SCCR} (g/mol) \times C_O (mol/L) \quad (10)$$

Where  $M_{SCCR}$  is the molar mass of SCCR dye (536.4 g/mol).

## Results and Discussion

### Characterization of PSH biosorbent

FESEM has been a primary tool that can reveal significant information about the surface morphology. FESEM analysis was employed in this study in order to characterize the surface morphology of PSH biosorbent material. The FESEM images for PSH are shown in Fig. 2. It can observe clear cavities with various sizes were distributed irregularly on the surface of the biosorbent particles. These scattered cavities are in the size ranging between 1-5  $\mu\text{m}$  (Fig. 2 (a)). Moreover, the high resolution FESEM image shows a rough surface with smaller pores that well distributed around the surface. These pores found in the PSH surface could be the main factor that had led to the high SCCR dye removal. The existence of these pores would enhance the surface area, which can provide more active sites

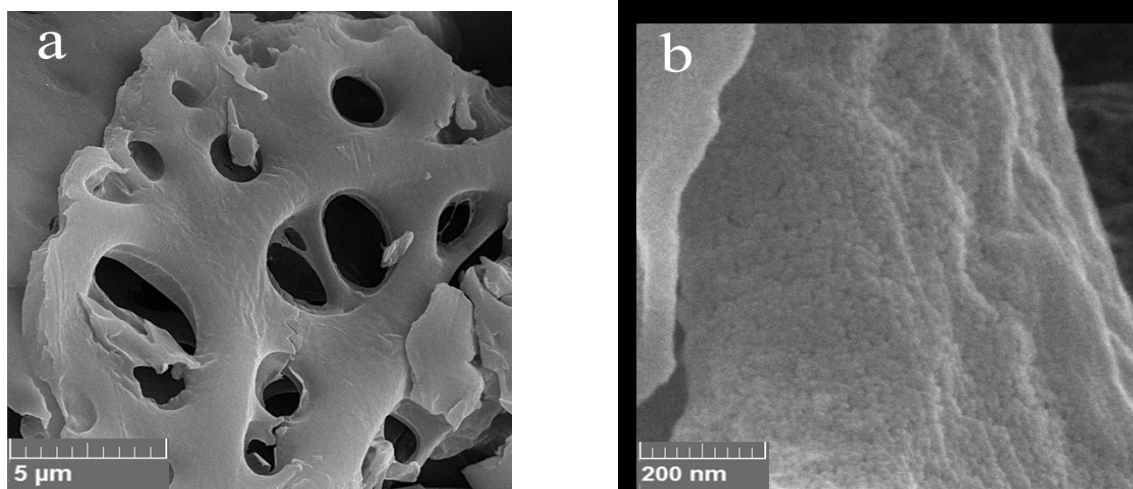


Fig. 2. FESEM images of PSH biosorbent material.

to permit better contact between the biosorbent surface and the dye molecules

#### Adsorption studies

Several adsorption parameters were studied to obtain the optimal adsorption conditions. The effect of the contact time on the adsorption of SCCR onto the PSH surface was examined between 10-180 min., 0.2 g biosorbent amount, 100 mg/L initial dye concentration, and at 25°C. From Figure 3, it can be observed a rise of adsorption efficiency values from 33% at 10 min. to 78% after 120 min., which can be related to the existence of a large number of adsorption active sites at the beginning of the adsorption process. Then it stabilized and no change occurred on the uptake level after that, which can be attributed to the decrease in the adsorption active sites on the biosorbent surface. This indicates that 120 min. is the optimal contact time to reach the equilibrium.

The effect of the PSH biosorbent dose on the adsorption of SCCR can be illustrated in Figure 4. It was investigated using various biosorbent amount of 0.01-0.3 g, 120 min. contact time, 100 mg/L initial dye concentration, and at 25°C. It can clearly see a low adsorption percentage of about 10% using low biosorbent dose, and as the biosorbent dose increases the adsorption efficiency increases to reach its maximum values of 78% using 0.2 g of the biosorbent. This can be explained by knowing that the uptake level highly depends on the availability of the adsorption sites on the PSH biosorbent surface. Increasing the PSH dose can supply additional adsorption sites to remove more dye particles from the solution, and thus increasing the adsorption level [36].

The effect of dye initial concentration on the adsorption process was also investigated using different initial dye concentrations of 25-150

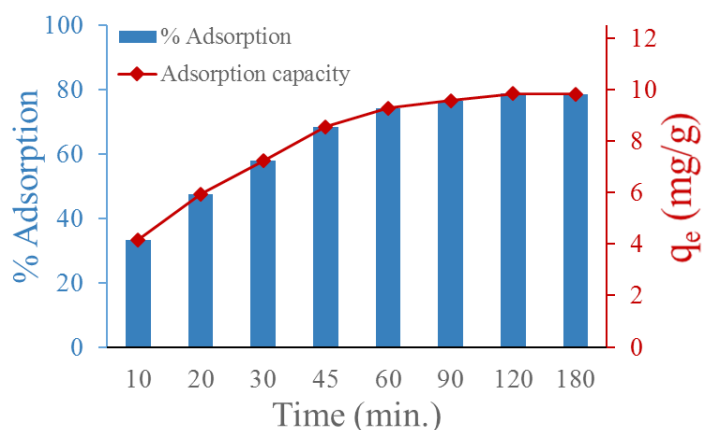


Fig.3. Effect of the contact time on the removal of SCCR onto PSH.

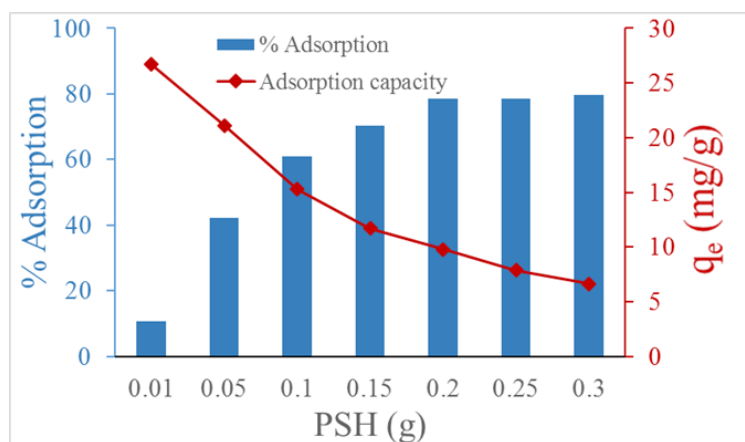


Fig. 4. Effect of the biosorbent amount on the removal of SCCR onto PSH.

mg/L, 120 min. contact time, 0.2 g biosorbent amount, and at 25°C. Figure 5 displays the effect of SCCR initial concentration on the adsorption of the dye onto the PSH biosorbent surface. It can be seen a good adsorption efficiency of about 73% at lower SCCR concentration, and as the dye concentration increases, the removal level increases to attain the highest level of 78% at 100 mg/L. Further increase in the dye concentration shows a decline in the adsorption efficiency, which can be attributed to the decrease in the vacant adsorption active sites that required to remove the dye particles [37]. On the other hand, an increase in the adsorption capacity of SCCR can be observed from 4.6 to 26.5 mg/g that can be attributed to the driving force generated from the concentration gradient at high PSH concentration [38].

#### Kinetic studies

The kinetic investigation for the removal of SCCR dye on PSH biosorbent was performed by applying three kinetic models. The adsorption data were analyzed using the pseudo-first order model [Eq. 3], pseudo-second order model (Eq. 4), and Intraparticle diffusion model (Eq. 5). The calculated parameters obtained from this analysis were presented in Table 1. The adsorption capacity ( $q_t$ ) and the pseudo-first order rate constant ( $k_1$ ) were calculated from the intercept and the slope of the linear plot of  $\ln(q_e - q_t)$  versus  $t$ . While the adsorption capacity and the pseudo-second order rate constant ( $k_2$ ) were obtained from the slope and intercept of the linear plot of  $t/q_t$  versus  $t$ . The values of the intraparticle rate constant ( $k_{in}$ ) and the intercept (C) were determined from the slope of the linear plot of  $q_t$  against  $t^{1/2}$ .

The calculated adsorption capacity value obtained using the pseudo-first order model does not fit well with the experimental value. Thus, the adsorption kinetic of SCCR does not follow this model. On the other hand, the calculated adsorption capacity obtained from applying the pseudo-second order model shows a more reasonable value that can give a better fit with the experimental value. Also, the correlation coefficient ( $R^2$ ) shows a greater value of 0.9976 for the pseudo-second order model, as can be seen from Table 1. This indicates that the adsorption of SCCR dye onto PSH surface follows the pseudo-second order kinetic model.

The results were further analyzed using the intraparticle diffusion model to investigate whether the intraparticle diffusion is the rate controlling step in adsorption of SCCR onto PSH. This model in most cases consists of three stages; the initial stage refers to the external mass transfer followed by an intermediate linear stage where intraparticle diffusion is the rate limiting. The final stage is the final equilibrium stage where intraparticle diffusion starts to slow down due to the extremely low adsorbate concentrations left in the solutions [39, 40]. If the intraparticle diffusion is the rate limiting step in the adsorption process, then the plots should be linear and the line passes across the origin [33].

The intraparticle diffusion plot of the amount of SCCR dye adsorbed versus the square root of time is presented in Figure 6. It can be seen that over the whole time range, the plot was not linear, implying that more than one process affected the adsorption [26].

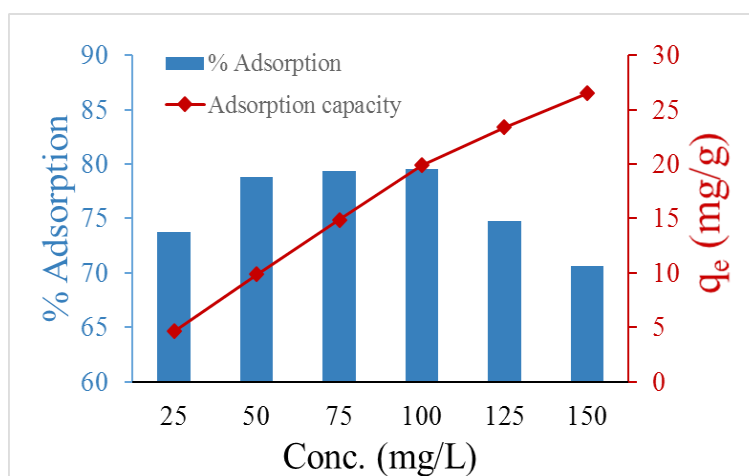


Fig. 5. Effect of the dye initial concentration on the removal of SCCR onto PSH.

TABLE 1: Kinetic parameters for the adsorption of SCCR onto PSH surface.

Kinetic model	Parameter	value
Pseudo-first order	$q_e$ exp. (mg. g <sup>-1</sup> )	9.828
	$q_e$ cal. (mg. g <sup>-1</sup> )	8.115
	$k_1$ (min <sup>-1</sup> )	0.0398
	R <sup>2</sup>	0.9808
Pseudo-second order	$q_e$ cal. (mg. g <sup>-1</sup> )	10.741
	$k_2$ (g. mg <sup>-1</sup> . min <sup>-1</sup> )	0.0069
Intraparticle diffusion	R <sup>2</sup>	0.9976
	$k_{int}$ (mg. g <sup>-1</sup> . min <sup>-1/2</sup> )	0.5326
	R <sup>2</sup>	0.7753

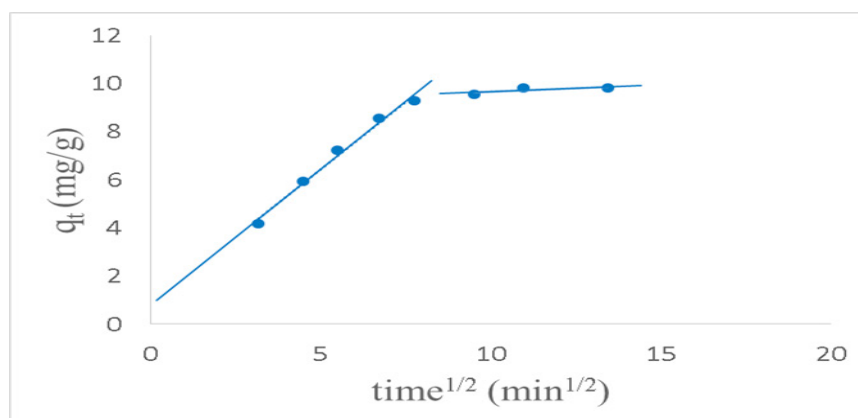


Fig.6. Intraparticle diffusion plot for the removal of SCCR onto PSH.

The absence of the first curved region of the initial stage in the plot suggests that the external surface adsorption is comparatively very fast and the intermediate stage of intraparticle diffusion is attained rapidly and continued to 80 min. Finally, the equilibrium adsorption stage starts after 90 min. The SCCR molecules are slowly diffuse into the adsorbent particles via intraparticle diffusion and retained in its pores. The results obtained agreed with those reported recently [41].

The intercept in this model gives an idea about the thickness of the boundary layer, and the larger the intercept, the greater the boundary layer effect [26]. The value of the correlation coefficient (R<sup>2</sup>) was 0.7753 that is much lower than that of pseudo-second order model.

#### Isothermal study

The effect Langmuir isotherm model was conducted for equilibrium data. It is well known that this model assumes a monolayer adsorption of the adsorbate molecules occurs on a homogenous adsorbent surface where the adsorption sites are energetically equivalent [42]. The applicability of Langmuir adsorption isotherm was examined for the removal of SCCR onto PSH. The linear plot using the Langmuir model (Eq. 6) is shown in Fig 7.

The Langmuir constants ( $q_m$  and  $K_l$ ) were derived from the intercept and the slope of the straight line obtained from the plot of  $1/q_e$  versus  $1/C_e$ . The maximum adsorption capacity was found to be 31.54 mg/g, while the Langmuir isotherm constant was 0.031943 L/mg. Moreover,

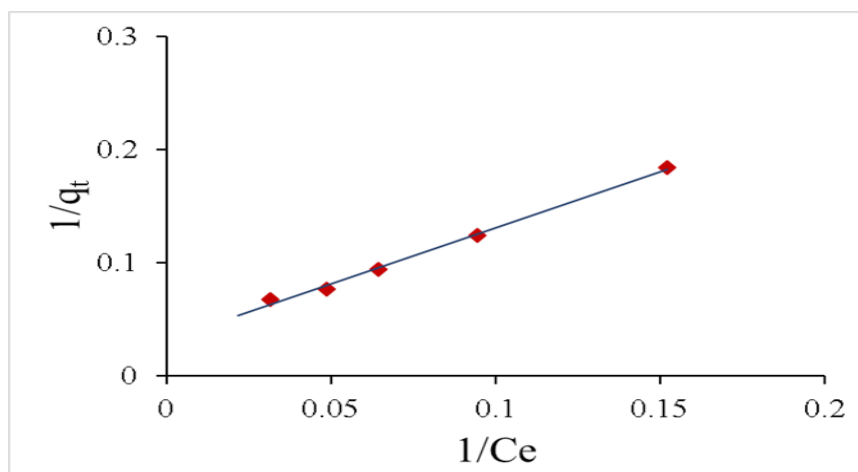


**Fig. 7. Langmuir adsorption isotherm for the removal of SCCR onto PSH.**

the analysis showed an excellent data fitting using the Langmuir model with the correlation coefficient  $R^2$  value of 0.99. Based on the high value correlation coefficient, it can be suggested that the removal of SCCR onto PSH follows the Langmuir isotherm. The fact that the Langmuir isotherm fits the experimental data very well may be due to the homogeneous distribution of active adsorption sites on PSH surface [33].

The main characteristic of the Langmuir model can be expressed in terms of the dimensionless constant separation factor  $R_L$  that can be defined by the following equation [43]:

$$R_L = 1 / (1 + K_L C_o)$$

Where  $C_o$  is the initial SCCR concentration (mg/L), and  $K_L$  (L/mg) is Langmuir constant. The value of  $R_L$  can be used to predict the type of the isotherm to be either irreversible ( $R_L = 0$ ), favorable ( $0 < R_L < 1$ ), linear ( $R_L = 1$ ) or unfavorable ( $R_L > 1$ ).

In this study, the determined  $R_L$  values for the removal of SCCR onto PSH were found to equal 0.3850, 0.2944, 0.2384, 0.2002 and 0.1276 at initial concentrations of 50, 75, 100, 125 and 150 mg/L, respectively. These values are between 0 and 1 that indicate the favorability of the adsorption process.

#### *Effect of Temperature and the Thermodynamic Studies*

The effect of temperature on the adsorption of the SCCR onto the PSH surface was plotted in Figure 8. It was examined at different temperatures ranged between 20-40 °C and using 120 min. contact time, 0.2 g biosorbent amount,

and 100 mg/L initial dye concentration. It can clearly see that the adsorption efficiency increased with increasing the temperature. It was increased from 74% to 83% as the temperature raised from 20 °C to 40 °C. Increasing the temperature may lead to decrease solution viscosity [44], and this can increase the ability of dye molecules to diffuse within the adsorbent micropores and adsorb onto the accessible adsorption active sites in the biosorbent surface, and thus increasing the removal efficiency. This result suggests the endothermic nature of the removal of SCCR onto the PSH surface.

The main thermodynamic functions were obtained by analyzing the experimental data between (20-40 °C) using equations (7-9).  $\Delta G^\circ$  was obtained using Eq. 7. Also,  $\Delta S^\circ$  and  $\Delta H^\circ$  were determined from the intercept and slope of the straight line acquired from Van't Hoff plot between  $\ln K$  versus  $1/T$ , respectively, as shown in Fig. 9.

The analyzed thermodynamic parameters for the adsorption of SCCR onto PSH surface at different temperatures are listed in Table 2. The removal process can be categorized as physical and chemical adsorption depending on the value of enthalpy change. If the value is less than 84 KJ/mol., then it classified as physical adsorption. Otherwise, the value between 84 to 420 KJ/mol. the chemical adsorption will take place [45, 46]. The positive value of  $\Delta H^\circ$  indicates that the removal process is endothermic [29]. Moreover, the magnitude of  $\Delta H^\circ$  found to be +121.567 KJ/mol., which reveals the chemical nature of the adsorption process. Furthermore, The positive value of  $\Delta S^\circ$  clarifies rising the randomness

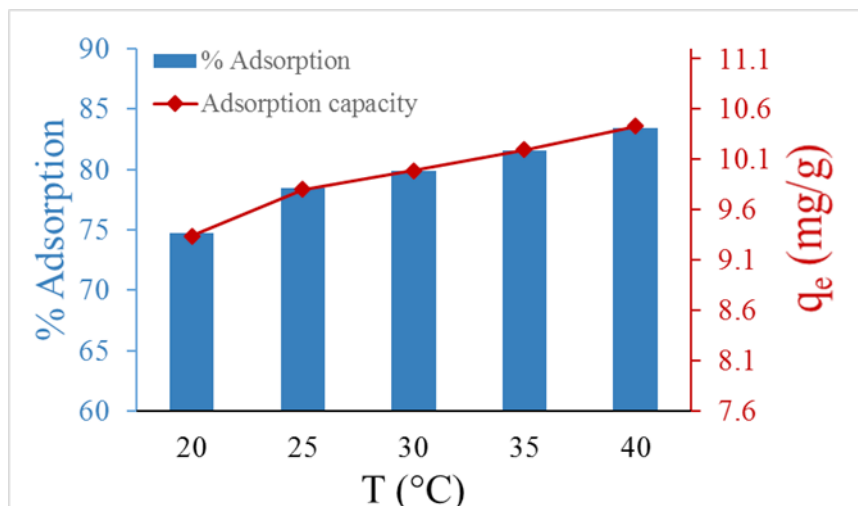


Fig. 8. Effect of the temperature on the removal of SCCR onto PSH.

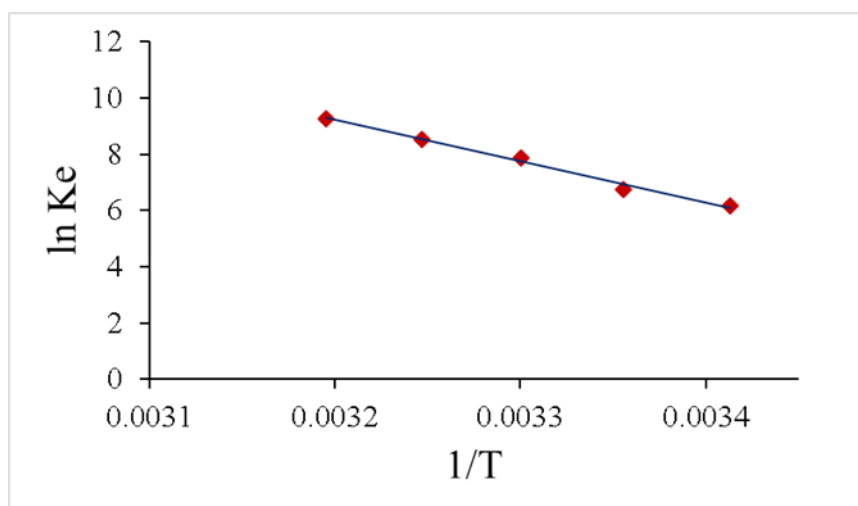


Fig. 9. Van't Hoff plot for SCCR adsorption on the PSH surface.

during the adsorption process at a solid-solution interface. In addition, the negative values of  $\Delta G^\circ$  elucidate the spontaneous nature of the adsorption process. Furthermore, the  $\Delta G^\circ$  values decreased with rising temperatures as can be noticed clearly in Table 2, which suggests that the removal process is more preferable at higher temperatures.

### Conclusions

This study examined the adsorption ability of Pumpkin seed husks as economic biosorbent material for the removal of Solochrome cyanine R from aqueous solutions. The effect of PSH biosorbent amount, contact time, initial SCCR concentration, and Temperature were investigated in order to obtain the optimal adsorption

conditions. The kinetic study suggests a good agreement of experimental data with the pseudo-second order model with a higher correlation coefficient. The evaluation of the adsorption data at different temperatures reveal the endothermic and randomness of the removal process. The  $\Delta G^\circ$  values indicate that the adsorption process has a temperature dependency with a spontaneous nature. These results proved that PSH could be an attractive alternative as adsorbent material for the removal of dyes from aqueous solutions.

### Acknowledgements

This research was supported by Tikrit University - Ministry of Higher Education and Scientific research, Iraq.

**TABLE 2: Thermodynamic parameters for the adsorption of SCCR onto PSH surface at different temperatures.**

T (°K)	$\Delta H^\circ$ (J/mol)	$\Delta S^\circ$ (J/mol <sup>-1</sup> . K)	$\Delta G^\circ$ (J/mol)	R <sup>2</sup>
293	121567.3	465.65	-15061.1	0.9905
298			-16722.2	
303			-19862.2	
308			-21852.7	
313			-24139.4	

**References:**

- Rosales E., Mejjide J., Tavares T., Pazos, M. and Sanromán, M.A., Grapefruit peelings as a promising biosorbent for the removal of leather dyes and hexavalent chromium. *Process Safety and Environmental Protection*, **101**, 61–71 (2016).
- Bhattacharyya K.G. and Sharma A., Azadirachta indica leaf powder as an effective biosorbent for dyes : a case study with aqueous Congo Red solutions. *Journal of Environmental Management*, **71**, 217–229 (2004).
- Seow T.W. and Lim C.K., Removal of dye by adsorption: A review. *International Journal of Applied Engineering Research*, **11**, 2675–2679 (2016).
- Kiernan J.A., Chromoxane cyanine R. I. Physical and chemical properties of the dye and of some of its iron complexes. *Journal of Microscopy*, **134**, 13–23 (1984).
- Ghaedi M., Heidari F., Kheirandish S., Dashtian K., Wang S. and Pourebrahim F., Chitosan extraction from lobster shells and its grafted with functionalized MWCNT for simultaneous removal of Pb 2+ ions and eriochrome cyanine R dye after their complexation. *International Journal of Biological Macromolecules*, **102**, 181–191 (2017).
- Singh N.B., Nagpal G. and Agrawal S., Environmental Technology & Innovation Water purification by using Adsorbents : A Review. *Environmental Technology & Innovation*, **11**, 187–240 (2018).
- Kandisa R.V., Kv N.S., Shaik K.B. and Gopinath R., Dye Removal by Adsorption : A Review. *Journal of Bioremediation & Biodegradation*, **7**, 371-374 (2016).
- Yagub M.T., Sen T.K., Afroze S. and Ang H.M., Dye and its removal from aqueous solution by adsorption: A review. *Advances in Colloid and Interface Science*, **209**, 172–184 (2014).
- Yu C. and Han X., Adsorbent Material Used In Water Treatment-A Review. *2nd International Workshop on Materials Engineering and Computer Sciences*, 290–293 (2015).
- Vasanth Kumar K. and Sivanesan S., Equilibrium data, isotherm parameters and process design for partial and complete isotherm of methylene blue onto activated carbon. *Journal of Hazardous Materials*, **134**, 237–244 (2006).
- Hameed B.H., Ahmad A.L. and Latiff K.N.A., Adsorption of basic dye ( methylene blue ) onto activated carbon prepared from rattan sawdust. *Dyes and Pigments*, **75**, 143–149 (2007).
- Ghaedi M., Shokrollahi A., Tavallali H., Shojaiepoor F., Keshavarz B., Hossainian H., Soylak M. and Purkait M.K., Activated Carbon and Multiwalled Carbon Nanotubes an Efficient Adsorbents for Kinetic and Equilibrium Study of Removal of Arsenazo ( III ) and Methyl Red Dyes from Waste Water. *Toxicological & Environmental Chemistry*, **93**, 438–449 (2011).
- Luna M.D.G., Flores E.D., Genuino D.A.D., Futralan C.M. and Wan M., Adsorption of Eriochrome Black T ( EBT ) dye using activated carbon prepared from waste rice hulls — Optimization , isotherm and kinetic studies. *Journal of the Taiwan Institute of Chemical Engineers*, **44**, 646–653 (2013).
- Konicki W., Sibera D., Mijowska E., Lenzion-Bieluń Z. and Narkiewicz U., Equilibrium and kinetic studies on acid dye Acid Red 88 adsorption by magnetic ZnFe<sub>2</sub>O<sub>4</sub> spinel

- ferrite nanoparticles. *Journal of Colloid and Interface Science*, **398**, 152–160 (2013).
15. Budiman H. and Zuas O., Adsorption isotherm studies on acid orange-10 dye removal using cerium dioxide nanoparticles. *Indonesian Journal of Chemistry*, **14**, 226–232 (2014).
  16. Al-Mahmoud S.M., Adsorption of Some Alephatic Dicarboxylic Acids on Zinc Oxide: A kinetic and Thermodynamic Study. *Baghdad Science Journal*, **16**, 892-897 (2019).
  17. Mouni L., Belkhirri L., Bollinger J-C., Bouzaza A., Assadi A., Tirri A., Dahmoune F., Madani K. and Remini H., Removal of Methylene Blue from aqueous solutions by adsorption on Kaolin: Kinetic and equilibrium studies, *Applied Clay Science*, **153**, 38–45 (2018).
  18. Castrillo N., Mercado A. and Volzone C., Sorption Water by Modified Bentonite. *Procedia Materials Science*, **8**, 391–396 (2015).
  19. Carazo E., Borrego-Sánchez A., Sánchez-Espejo R., García-Villén F., Cerezo P., Aguzzi C. and Viseras C., Kinetic and thermodynamic assessment on isoniazid/montmorillonite adsorption. *Applied Clay Science*, **165**, 82–90 (2018).
  20. Sadri S., Johnson B.B., Ruyter-Hooley M. and Angove M.J., The adsorption of nortriptyline on montmorillonite, kaolinite and gibbsite. *Applied Clay Science*, **165**, 64–70 (2018).
  21. Temesgen F., Gabbiye N. and Sahu O., Biosorption of Reactive Red Dye (RRD) on Activated Surface of Banana and Orange Peels: Economical Alternative for Textile Effluent. *Surfaces and Interfaces*, **12**, 151–159 (2018).
  22. Abdel Ghafar H., Salama M. and Radwan E.K., Salem T., Recycling of pre-consumer viscose waste fibers for the removal of cationic dye from aqueous solution, *Egyptian Journal of Chemistry*, **62**, 1457–1467 (2019).
  23. Romero-Canoa L.A., González-Gutiérrez L .V., Baldenegro-Pérez L.A. and Marín F.C., Grapefruit peels as biosorbent: characterization and use in batch and fixed bed column for Cu(II) uptake from wastewater. *Journal of Chemical Technology Biotechnology*, **72**, 1650–1658 (2017).
  24. Vadivelan V. and Kumar K.V., Equilibrium , kinetics , mechanism , and process design for the sorption of methylene blue onto rice husk. *Journal of Colloid and Interface Science*, **286**, 90–100 (2005).
  25. Al-husseiny H.A., Adsorption of Methylene Blue Dye Using Low Cost Adsorbent of Sawdust : Batch and Continues Studies. *Journal of Babylon University/Engineering Sciences*, **22**, 296–310 (2014).
  26. Hameed B.H., Spent tea leaves: A new non-conventional and low-cost adsorbent for removal of basic dye from aqueous solutions. *Journal of Hazardous Materials*, **161**, 753–759 (2009).
  27. Etim U.J., Umoren S.A. and Eduok U.M., Coconut coir dust as a low cost adsorbent for the removal of cationic dye from aqueous solution. *Journal of Saudi Chemical Society*, **20**, S67–S76 (2016).
  28. Hameed B.H. and El-Khaiary M.I., Removal of basic dye from aqueous medium using a novel agricultural waste material: Pumpkin seed hull. *Journal of Hazardous Materials*, **155**, 601–609 (2008).
  29. Subbaiah M.V. and Kim D.S., Adsorption of methyl orange from aqueous solution by aminated pumpkin seed powder: Kinetics, isotherms, and thermodynamic studies. *Ecotoxicology and Environmental Safety*, **128**, 109–117 (2016).
  30. Barrett E.P., Joyner E.G. and Halenda P.P., The Determination of Pore Volume and Area Distributions in Porous Substances. I. Computations from Nitrogen Isotherms. *Journal of the American Chemical Society*, **73**, 373–80 (1951).
  31. Ho Y.S. and Mckay G., Sorption of dye from aqueous solution by peat. *Chemical Engineering Journal*, **70**, 115–24 (1998).
  32. Weber W.J. and Morris J.C., Kinetics of Adsorption on Carbon from Solution. *Journal of the Sanitary Engineering Division*, **89**, 31–60 (1963).
  33. Hameed B.H., Mahmoud D.K. and Ahmad A.L., Sorption of basic dye from aqueous solution by pomelo (Citrus grandis) peel in a batch system. *Colloids and Surfaces A: Physicochemical and Engineering Aspects*, **316**, 78–84 (2008).
  34. Langmuir I., The adsorption of gases on plane surfaces of glass, mica and platinum. *Journal of the American Chemical Society*, **40**, 1361–1403 (1918).
  35. Atkins P. and Paula J.d., *Physical chemistry*, 8th Ed., W. H. Freeman and Company, New York (2006).
  36. Salleh M.A.M., Mahmoud D.K., Karim

- W.A.W.A. and Idris A., Cationic and anionic dye adsorption by agricultural solid wastes: A comprehensive review. *Desalination*, **280**, 1–13 (2011).
37. Barka N., Qourzal S., Assabbane A., Nounah A. and Ait-Ichou Y., Removal of Reactive Yellow 84 from aqueous solutions by adsorption onto hydroxyapatite. *Journal of Saudi Chemical Society*, **15**, 263–267 (2011).
38. Pal A., Pan S. and Saha S., Synergistically improved adsorption of anionic surfactant and crystal violet on chitosan hydrogel beads. *Chemical Engineering Journal*, **217**, 426–434 (2013).
39. Cheung W.H., Szeto Y.S. and McKay G., Intraparticle diffusion processes during acid dye adsorption onto chitosan. *Bioresource Technology*, **98**, 2897–2904 (2007).
40. Daifullah A.A., Yakout S.M. and Elreefy S.A., Adsorption of fluoride in aqueous solutions using KMnO<sub>4</sub>-modified activated carbon derived from steam pyrolysis of rice straw. *Journal of Hazardous Materials*, **147**, 633–43 (2007).
41. Omri A., Wali A. and Benzina M., Adsorption of bentazon on activated carbon prepared from Lawsonia inermis wood: Equilibrium, kinetic and thermodynamic studies, *Arabian Journal of Chemistry*, **9**, S1729–39 (2016).
42. Khobragade M.U. and Pal A., Investigation on the adsorption of Mn ( II ) on surfactant-modified alumina : Batch and column studies. *Journal of Environmental Chemical Engineering*, **2**, 2295–305 (2014).
43. Hall K.R., Eagleton L.C., Acrivos A. and Vermeulen T., Pore-and solid-diffusion kinetics in fixed-bed adsorption under constant-pattern conditions. *Industrial and Engineering Chemistry Fundamentals*, **5**, 212–223 (1966).
44. Halbus A.F., Salman J.M., Lafta A.J., Athab Z.H., Hasan F.M., Kamil A.M. and Hussein F.H., Equilibrium, isotherms and thermodynamic studies of Congo red adsorption onto ceratophyllum demersum. *Indian Journal of Chemical Technology*, **24**, 82–87 (2017).
45. Errais E., Duplay J., Darragi F., Rabet I.M., Aubert A., Huber F. and Morvan G., Efficient anionic dye adsorption on natural untreated clay : Kinetic study and thermodynamic parameters. *Desalination*, **275**, 74–81 (2001).
46. Alver E. and Metin A., Anionic dye removal from aqueous solutions using modified zeolite: Adsorption kinetics and isotherm studies. *Chemical Engineering Journal*, **200–202**, 59–67 (2012).

### دراسة حركية وايزوثرمية وثرموداينميكية لاستخدام قشور بذور اليقطين كمادة حيوية واطنة التكلفة لامتزاز صبغة Solochrome cyanine R من المحاليل المائية

صدام محمد المحمود

قسم الكيمياء، كلية التربية للبنات، جامعة تكريت، تكريت، العراق.

استخدمت قشور بذور اليقطين في هذا البحث كمادة فعالة منخفضة التكلفة لامتزاز صبغة Solochrome cyanine R من المحاليل المائية. ولقد لوحظ القابلية الجيدة لهذه القشور على إزالة الصبغة. كما وجد ان ظروف الامتزاز المثلى كانت عند ١٢٠ دقيقة الزمن اللازم للامتزاز، ٠,٢ غم من المادة المازة، و ١٠٠ ملغم/لتر التركيز الابتدائي للصبغة. أظهرت حركيات الامتزاز ان تطبيق نموذج معادلة السرعة من الدرجة الثانية الكاذبة يعطي افضل وصف لعملية الامتزاز مع اعلى قيمة لمعامل الارتباط. اعطى تطبيق معادلة لنكير على النتائج وصف ممتاز مع استنتاج ان عملية الامتزاز كانت مفضلة. تم تقييم نتائج عملية الامتزاز عند درجات حرارية مختلفة وذلك للحصول على قيم المعاملات الثرموداينميكية. تشير القيم الإيجابية لكل من التغير في الإنثالبي والتغير في الإنتروبي الى الطبيعة الماصة للحرارة وزيادة العشوائية لعملية الامتزاز. إضافة لذلك، فان القيم السالبة للتغير في طاقة جيبس الحرة تشير الى تلقائية عملية الامتزاز كما انها أكثر تفضيلاً عند درجات الحرارة الأعلى. من خلال هذه النتائج يتبين ان استخدام قشور بذور اليقطين كمادة مازة حيوية واطنة التكلفة تظهر إمكانية كبيرة لامتزاز صبغة Solochrome cyanine R من المحاليل المائية.